Stopped-Flow Kinetic Study of the Complex Formation between Pyridoxal 5′-Phosphate and Bovine Serum Albumin

Kiyofumi MURAKAMI,* Yukio KUBOTA, Yasuo FUJISAKI, and Takayuki SANO†
Department of Chemistry, Faculty of Science, Yamaguchi University,
Yoshida 1677-1, Yamaguchi 753
†Department of Chemistry, Faculty of Science, Hiroshima University,
Higashisenda-machi, Naka-ku, Hiroshima 730
(Received May 15, 1986)

The complex formation between pyridoxal 5′-phosphate (PLP) and bovine serum albumin at pH=7.0 and 25 °C was characterized by four relaxation processes. The dependence of the reciprocal relaxation times upon reactant concentrations was found to be consistent with a mechanism in which a rapid bimolecular binding step is followed by three sequential isomerization steps. The eight rate constants for this mechanism were determined and then combined to calculate an overall equilibrium constant which is in agreement with the literature value. Absorption spectra of the complexes formed by the two faster steps were determined from absorbance changes associated with them; the spectrum corresponding to the first complex has two bands at 330 nm and 360 nm and an additional 410 nm band, while the spectrum corresponding to the second complex has a large single band at 375 nm. Comparing these spectra with those reported for other PLP-enzyme systems, we speculate that four steps in the proposed mechanism may correspond to the rapid formation of a carbinolamine, which is in very rapid equilibrium with a Schiff base form, followed by the deprotonation of the ring nitrogen, the formation of an ionic hydrogen-bonded Schiff base, and the final formation of a nonionic hydrogen-bonded Schiff base.

Pyridoxal 5′-Phosphate (PLP), which is an important cofactor of many enzymes, has been found to be transported in plasma by albumin molecules.[1] Dempsey and Christensen[2] have studied the binding of PLP with bovine serum albumin (BSA) and have shown that there are at least two kinds of strong binding sites, i.e., the primary site characterized by the 332 nm absorption band and the association constant $K_{ass}>10^6$ M^{-1} †† and the secondary site characterized by the 415 nm band and $K_{ass}\sim10^5$ M^{-1}. The bindings occur at ε-amino lysine groups of the protein. On the basis of the irreducibility by $NaBH_4$ and the abundance of lysyl residues in the neighborhood of the primary binding site, Dempsey and Christensen[2] and Anderson et al.[3] have suggested that the structure of PLP bound to the primary site is not a Schiff base but a substituted aldimine. On the other hand, recent polarographic[4] and circular dichroism[5] studies have claimed that a nonionic hydrogen-bonded Schiff base structure is responsible for the primary complex. Although this structure seems to be plausible, the process of its formation has not been well elucidated.

The present study describes the kinetics of the interaction of PLP with BSA. Our goal is to establish an overall reaction mechanism for the binding of PLP to the primary site.

Experimental

Materials. Albumin (fraction V from bovine serum) was purchased from Wako Pure Chemical Industries and used without further purification. The dimer content was about 5%. The molar concentration of BSA was determined from the absorbance at 280 nm ($E^{1\%}_{1\,cm}=6.6$[6]), assuming its molecular weight of 67000. Pyridoxal 5′-phosphate was purchased from Tokyo Kasei and used without further purification. All the sample solutions were prepared in 0.1 M phosphate buffer at pH=7.00±0.02.

Methods. Absorption spectra were measured with a Union Giken SM401 Spectrophotometer. Kinetic measurements were performed using a Union Giken stopped-flow apparatus (RA401 and RA1100). In order to investigate the binding to the primary site all the measurements were carried out at P_0/L_0 (protein to ligand ratio)≧1. The temperature was controlled to be 25±0.2 °C.

Results and Discussion

Relaxations and Their Characteristics. The stopped-flow and spectrophotometric measurements revealed that the binding of PLP to BSA occurs through four distinct relaxations. Typical traces observed are shown in Fig. 1. Among these, the two slower relaxations have already been reported by Dempsey and Christensen.[2] They showed that an increase of absorbance around 415 nm within 100 s is followed by a very slow increase of that at 332 nm with a loss of the 415 nm band, exhibiting an apparent isosbestic point at 350 nm. However, the two faster relaxations have not been reported so far.

The relaxation time (τ) for each relaxation was determined from a semi-logarithmic plot of the trace. Figures 2—5 show the concentration dependence of the reciprocal relaxation times. As can be seen in Figs. 4(A) and 5(A), the concentration dependence of τ^{-1} at $L_0=5\times10^{-5}$ M for each of the two slower relaxations exhibits a sharp increase within a narrow range of the protein concentration above $P_0=5\times10^{-5}$ M. Only with these data it is difficult to perform an accurate determination of kinetic parameters. Hence, the concentration dependence of τ^{-1} at $P_0/L_0=1$ (Figs.

†† 1 M=1 mol dm^{-3}.

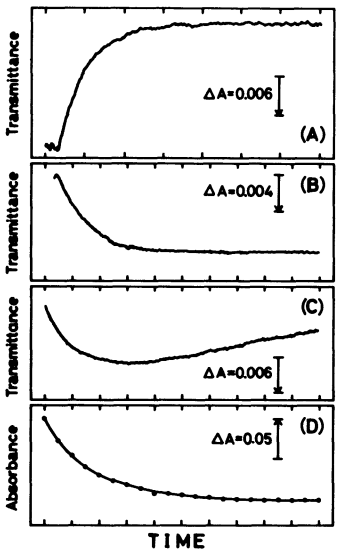

Fig. 1. Typical traces of the reaction observed after the mixing of PLP (1×10^{-4} M) and BSA (1×10^{-4} M). (A): Transmittance change at 390 nm. (B): Transmittance change at 390 nm. (C): Transmittance change at 415 nm. (D): Absorbance change at 415 nm. The abscissa scale is (A) 2.5 ms per division, (B) 100 ms per division, (C) 100 s per division, and (D) 1 h per division. The three faster relaxations were observed by the stopped-flow method, while the fourth one by spectrophotometry. The arrow designated for each trace shows the magnitude and the direction of the positive absorbance change.

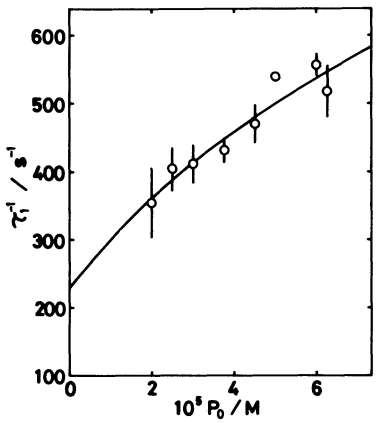

Fig. 2. Concentration dependence of τ_1^{-1} at P_0/L_0 (protein to ligand ratio)=1. The abscissa indicates the initial concentration after mixing. The solid line represents the theoretical curve calculated using the equilibrium and rate constants listed in Table 1. Legends are also the case for Figs. 3—5.

4(B) and 5(B)), which exhibits a more gradual increase with protein concentration, was also measured and analyzed together with the previous data. τ_1^{-1} increases progressively with an increase in the protein concentration, while τ_2^{-1}, τ_3^{-1}, and τ_4^{-1} increase at low concentrations but tend toward constant values at

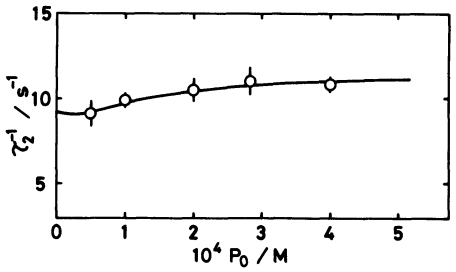

Fig. 3. Concentration dependence of τ_2^{-1} at $L_0=5\times10^{-5}$ M.

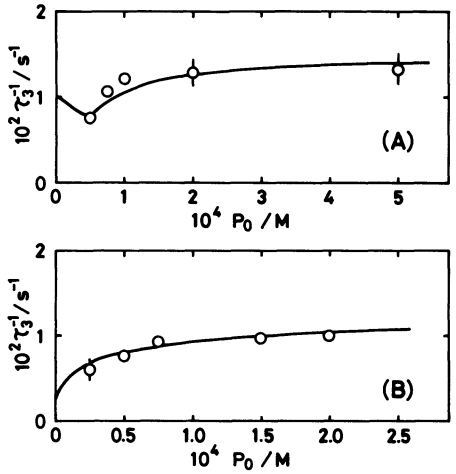

Fig. 4. Concentration dependence of τ_3^{-1}. (A) Concentration dependence at $L_0=5\times10^{-5}$ M. (B) Concentration dependence at $P_0/L_0=1$.

high concentrations. This behavior suggests a reaction scheme that a bimolecular rapid binding step is followed by three sequential isomerization reaction steps.

Reaction Scheme. In order to interpret the concentration dependence of the reciprocal relaxation times, the following model is examined.

$$\mathbf{L}+\mathbf{P} \underset{k_{-1}}{\overset{\overset{K_1}{k_1}}{\rightleftarrows}} \mathbf{C}_1 \underset{k_{-2}}{\overset{\overset{K_2}{k_2}}{\rightleftarrows}} \mathbf{C}_2 \underset{k_{-3}}{\overset{\overset{K_3}{k_3}}{\rightleftarrows}} \mathbf{C}_3 \underset{k_{-4}}{\overset{\overset{K_4}{k_4}}{\rightleftarrows}} \mathbf{C}_4, \tag{1}$$

where **L**, **P**, and **C** denote free ligand, free protein and complex species, respectively, and K_i, k_i, and k_{-i} are the equilibrium constant, the forward and backward rate constants of the ith step. This mechanism predicts four relaxation times, defined by

$$\tau_1^{-1} = k_1(L+P) + k_{-1}, \tag{2}$$

$$\tau_2^{-1} = k_2\frac{K_1(L+P)}{1+K_1(L+P)} + k_{-2}, \tag{3}$$

$$\tau_3^{-1} = k_3\frac{K_1K_2(L+P)}{1+K_1(1+K_2)(L+P)} + k_{-3}, \tag{4}$$

$$\tau_4^{-1} = k_4\frac{K_1K_2K_3(L+P)}{1+K_1\{1+K_2(1+K_3)\}(L+P)} + k_{-4}, \tag{5}$$

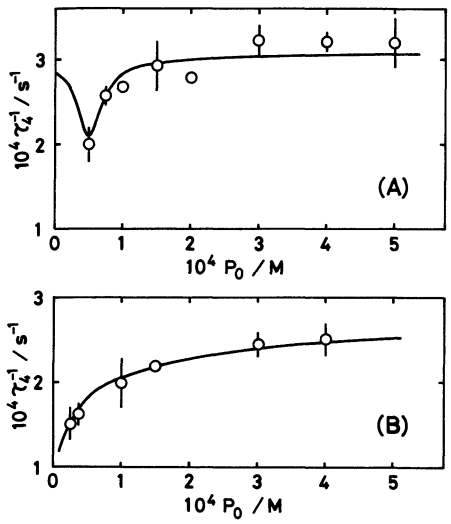

Fig. 5. Concentration dependence of τ_4^{-1}. (A) Concentration dependence at $L_0=5\times10^{-5}$ M (B) Concentration dependence at $P_0/L_0=1$.

where L and P, respectively, denote free ligand and free protein concentrations at the end of each step and where the rapid equilibrium of the preceding step has been assumed in each case, since the relaxation times observed for the present system are well separated each other (Fig. 1).

The data of Figs. 2—5 were fitted to Eqs. 2—5 by linear or nonlinear regression analysis, using the following protocol. First, an arbitrary K_1 was chosen to calculate the equilibrium concentrations, L and P, at the end of the first step. Then the best straight-line fit of τ_1^{-1} vs. $(L+P)$ was found to obtain k_1, k_{-1}, and K_1. The procedure was iterated until all the parameters converge. The estimate of K_1 was used with Eq. 3 to fit the data of Fig. 3 and to obtain k_2, k_{-2}, and K_2. The estimated values for K_1 and K_2 were used with Eq. 4 to obtain k_3, k_{-3}, and K_3 from the data of Fig. 4. Finally, k_4, k_{-4}, and K_4 were determined using Eq. 5 and the data of Fig. 5. The solid lines in Figs. 2—5 indicate the best least-squares fits, and the kinetic parameters obtained are summarized in Table 1.

The overall association constant for Scheme 1 is given by

$$K_{ass} = K_1(1+K_2+K_2K_3+K_2K_3K_4). \quad (6)$$

From the kinetic data of Table 1, we calculate an overall association constant of 5.27×10^6 M^{-1}. This value is consistent with the prediction by Dempsey and Christensen[2] that K_{ass} for the primary site should be larger than 1×10^6 M^{-1}. Independently of the first step, K_1 can be estimated by nonlinear regression analysis using Eq. 3 and the data of Fig. 3. The result is $K_1=2.02\times10^4$ M^{-1}, a value in excellent agreement with the estimate of K_1 in Table 1. The agreement of these values lends considerable confidence to the validity of Scheme 1 as a plausible reaction scheme.

Table 1. Equilibrium and Rate Constants Associated with the Mechanism of Eq. 1

Step	K_i	k_i	$\frac{k_{-i}}{s^{-1}}$
1	1.94×10^4 M^{-1}	4.41×10^6 M^{-1} s^{-1}	227
2	0.702	4.77 s^{-1}	6.80
3	13.5	3.03×10^{-2} s^{-1}	2.25×10^{-3}
4	27.5	3.49×10^{-4} s^{-1}	1.27×10^{-5}

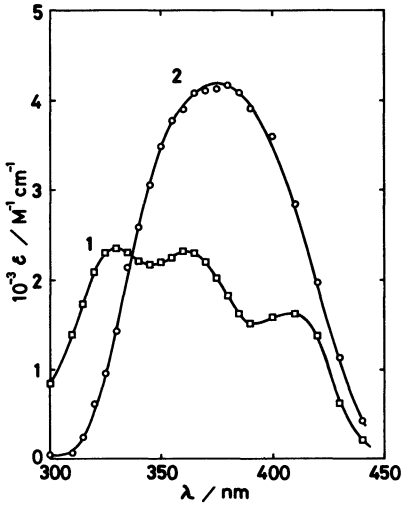

Fig. 6. Absorption spectra of $\mathbf{C}_1$ (curve 1) and $\mathbf{C}_2$ (curve 2).

Structures of the Intermediate Species. To investigate the structures of the intermediate species in Scheme 1, the molar extinction coefficients were determined as follows. At the end of the first step, the absorbance of the sample at a given wavelength can be expressed by

$$A_1 = \varepsilon_L L + \varepsilon_P P + \varepsilon_1 C_1, \quad (7)$$

where ε_L, ε_P, and ε_1 are molar extinction coefficients of the free ligand, the free protein and the first complex, respectively. Using the change in absorbance associated with the first step (ΔA_1), A_1 can also be expressed as

$$A_1 = A_0 + \Delta A_1, \quad (8)$$

where A_0 is the absorbance of the sample after mixing but before initiation of the reaction. Combining Eqs. 7 and 8, ε_1 becomes

$$\varepsilon_1 = \frac{A_0+\Delta A_1-\varepsilon_L L-\varepsilon_P P}{C_1}. \quad (9)$$

In this equation, ε_L, ε_P, and A_0 can be estimated from spectrophotometric data for the reactants, and the concentrations L, P, and C_1 can be calculated with the value of K_1 in Table 1. ΔA_1 was determined taking into account the dead time of the apparatus. Sub-

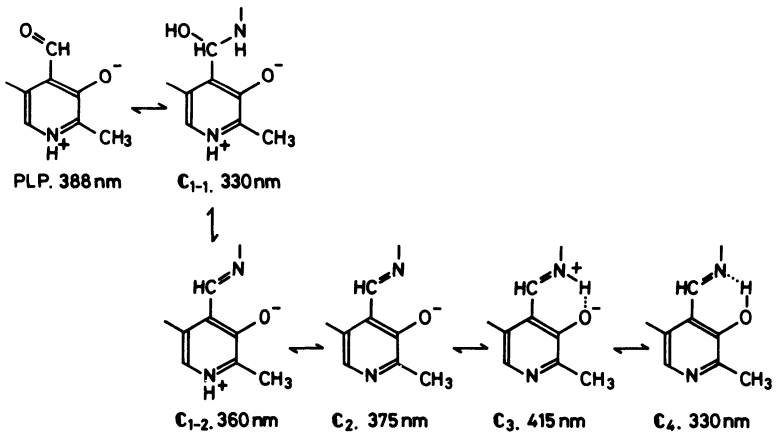

Fig. 7. Mechanism for the isomerization of PLP at the primary site.

stitution of these values into Eq. 9 yields the molar extinction coefficient of C_1 (ε_1). The molar extinction coefficient of C_2 (ε_2) was also determined in a similar manner. The absorption spectra of C_1 and C_2 thus obtained are displayed in Fig. 6. The absorption spectra of C_1 (curve 1) has two maxima at 330 nm and 360 nm and a small peak around 410 nm, suggesting the existence of more than one spectral species, while that of C_2 (curve 2) exhibits a single strong band having a peak at 375 nm. These 360 and 375 nm bands have not been reported for the PLP-albumin system.

Considering the present kinetic data and other results reported so far, we propose a mechanism for the complex formation at the primary site (Fig. 7). Three possible structures, i.e., substituted aldimine,[2,7] carbinolamine[2] and nonionic hydrogen-bonded Schiff base,[4,5,8] have been proposed for 330 nm band. Among these the carbinolamine (C_{1-1}) is the most suitable structure for the 330 nm band in curve 1 of Fig. 6 because it is an intermediate structure[9] for a subsequent Schiff base formation. The 360 nm band, which has been observed as a stable species for PLP-aspartate β-decarboxylase[10] and PLP-aspartate aminotransferase[11-15] systems, is now generally recognized as due to a Shiff base structure (C_{1-2}). Considering that the relaxation time for the formation of C_{1-1} was indistinguishable from that of C_{1-2}, it seems reasonable to conclude that these structures are in very rapid equilibrium with each other.

Matsushima and Martell[16] have observed a single strong band for pyridoxylidenevaline (373 nm) and pyridoxal phosphate valine Schiff base (350 nm) in alkaline methanol solutions, and assigned the band to the π_1 band of the anionic form of the Schiff base. The resemblance of the present absorption spectrum (curve 2 in Fig. 6) to those bands suggests that the anionic Schiff base structure is responsible for C_2.

The 415 nm band is attributed to an ionic hydrogen bonded Schiff base structure (C_3), with or without protonation of the ring nitrogen.[3,4,16,17] Considering that the ring nitrogen is already deprotonated in the previous step ($C_{1-2} \rightarrow C_2$), it is reasonable to expect that the ring nitrogen of C_3 is deprotonated rather than protonated.[8] The appearance of the band around 410 nm in curve 1 of Fig. 6 implies the existence of another path of the rapid formation of an ionic hydrogen-bonded Schiff base at a different site, which may correspond to the secondary site.

Based on the irreducibility of the complex by $NaBH_4$ and the presence of three lysyl residues in the neighborhood of the primary binding site, Dempsey and Christensen[2] and Anderson et al.[3] have suggested a substituted aldimine, in which the ring nitrogen is protonated, for the final and stable complex (330 nm band). However, the mechanism shown in Fig. 7 suggests that the nonionic hydrogen-bonded Schiff base in hydrophobic environment rather than the substituted aldimine is plausible for C_4. It is likely that the hydrophobic environment causes the irreducibility of the Schiff base by $NaBH_4$. This structure is consistent with the conclusion obtained from polarographic studies[4] and circular dichroism and spectrophotometric investigations.[5,8] The proposed mechanism (Fig. 7) indicates that the structure of bound PLP changes, step by step, from the polar form to the nonpolar one. Perhaps PLP first binds to a polar site at the surface of the protein and migrates to a more hydrophobic region.

The authors wish to express their thanks to Professor Tatsuya Yasunaga of Kinki University for his helpful discussions.

References

1) L. Lumeng, R. E. Brashear, and Y.-K. Li, *J. Lab. Clin. Med.*, **84**, 334 (1974).

2) W. B. Dempsey and H. N. Christensen, *J. Biol. Chem.*, **237**, 1113 (1962).

3) J. A. Anderson, H.-F. W. Chang, and C. J. Granjean, *Biochemistry*, **10**, 2408 (1971).

4) M. Cortijo, J. S. Jimenez, and J. Llor, *Biochem. J.*, **171**, 497 (1978).
5) S. Shimomura and T. Fukui, *J. Biochem.*, **81**, 1781 (1977).
6) E. J. Cohn, W. L. Huges, Jr., and J. H. Weare, *J. Am. Chem. Soc.*, **69**, 1753 (1947).
7) A. B. Kent, E. G. Krebs, and E. H. Fischer, *J. Biol. Chem.*, **232**, 549 (1958).
8) M. C. Hilak, B. J. M. Harmsen, J. J. M. Joordens, and G. A. J. Van Os, *Int. J. Peptide Protein Res.*, **7**, 411 (1975).
9) D. S. Auld and T. C. Bruice, *J. Am. Chem. Soc.*, **89**, 2083 (1967).
10) E. M. Wilson and A. Meister, *Biochemistry*, **5**, 1166 (1966).
11) W. T. Jenkins and I. W. Sizer, *J. Am. Chem. Soc.*, **79**, 2655 (1957).
12) Y. N. Breusov, V. I. Ivanov, M. Y. Karpeisky, and Y. V. Morozov, *Biochim. Biophys. Acta*, **92**, 388 (1964).
13) M. Martinez-Carrion, D. C. Tiemeier, and D. L. Peterson, *Biochemistry*, **9**, 2574 (1970).
14) S. M. Bonsib, R. C. Harruff, and W. T. Jenkins, *J. Biol., Chem.*, **250**, 8635 (1975).
15) D. E. Metzler, *Adv. Enzymol. Relat. Areas. Mol. Biol.*, **50**, 1 (1979).
16) Y. Matsushima and A. E. Martell, *J. Am. Chem. Soc.*, **89**, 1322 (1967).
17) G. F. Johnson, J.-I. Tu, M. L. S. Bartlett, and D.J. Graves, *J. Biol. Chem.*, **245**, 5560 (1970).